

## Effects of terrain on the occurrence of debris flows after forest harvesting

メタデータ	言語: eng 出版者: 公開日: 2021-06-14 キーワード (Ja): キーワード (En): 作成者: Imaizumi, Fumitoshi, Sidle, Roy C. メールアドレス: 所属:
URL	<a href="http://hdl.handle.net/10297/00028265">http://hdl.handle.net/10297/00028265</a>

# **Effects of terrain on occurrence of debris flows after forest harvesting**

Fumitoshi Imaizumi<sup>a\*</sup> and Roy. C. Sidle<sup>b</sup>

*<sup>a</sup>Faculty of Agriculture, Shizuoka University, Shizuoka, Japan; <sup>b</sup>Mountain Societies Research Institute and Earth and Environmental Sciences Department, University of Central Asia, Khorog, Tajikistan*

\*corresponding author: [imaizumi@shizuoka.ac.jp](mailto:imaizumi@shizuoka.ac.jp)

# Effects of terrain on occurrence of debris flows after forest harvesting

Forest harvesting and subsequent forest regeneration represent widespread changes in land cover in mountain regions. Although impacts of forest harvesting on landslide initiation has been widely reported, the effects of forest harvesting on the occurrence of debris flows remains unclear. We propose that forest harvesting will differentially affect the susceptibility of debris flows amongst catchments with different terrain characteristics. This hypothesis was assessed in the Sanko catchment, Japan, where comprehensive forest harvest records date back to 1913. The frequency of debris flows directly originating from landslides occurred in similar timeframes as the occurrence of landslides. Landslides that reached channels and continued downstream as debris flows were more prevalent in steep channel reaches with small hillslope-channel junction angles. In addition to the increase in frequency of landslides, especially within 10 years after forest harvesting, debris flows caused by mass movement of channel deposits in steep reaches increased during this period. These relationships between occurrence of debris flows and channel topography indicate a high susceptibility of debris flow occurrence after forest harvesting in first and zero-order mountain streams. Sediment previously routed into channel networks by landslides is likely a more important factor for in-channel debris flow initiation in the lower channel reaches, while instability of areas proximate to riparian zones, including stream banks and geomorphic hollows, possibly accelerate occurrence of debris flows in upper channel reaches. Consequently, catchment topography should be considered in evaluating debris flow risk after forest harvesting.

Keywords: word; forest harvesting; debris flow; landslide; sediment supply; sediment disasters

## Introduction

Debris flows are natural hydrogeomorphic processes in steep terrain that continuously shape headwater channels and downstream landforms, but when humans, infrastructure, and property are located in debris flow inundation areas, major disasters can occur (Bovis and Jakob, 1999; Jakob et al., 2005; Imaizumi et al., 2019). Forest harvesting and subsequent forest regeneration represent widespread land cover changes that affect

sediment transport on mountain hillslopes (Sidle and Wu, 1999; Ueno et al., 2015; Schmaltz et al., 2017). Numerous studies worldwide quantify the impacts of forest harvesting on the susceptibility of sediment transport processes. Landslide frequency increases after forest harvesting (Jacob, 2000; Montgomery et al., 2000; Brardinoni et al., 2002; Guthrie, 2002; Sidle and Ochiai, 2006; Saito et al., 2017) because decay of root networks decrease shear resistance of soil (Sidle, 1992; Sakals and Sidle, 2004; Vergani et al., 2017). In addition, logging roads and skid trails disturb forest soils and activate surface erosion (Jordan, 2006; Sidle et al., 2006; Ziegler et al., 2006). Previous studies have mainly evaluated impacts of the forest harvesting on hydrogeomorphic processes in unstable terrain. In contrast, ambiguity still remains concerning the impacts of harvesting on the occurrence of debris flows (May, 2002; Jakob et al., 2005; Imaizumi, 2019).

Increases in debris flow frequency are associated with increased landslide occurrence in steep terrain because many landslides directly evolve into debris flows (Fan et al., 2017). Additionally, increases in stream discharge during intense rainfall events trigger debris flows originating within stream channels (Kean et al., 2013; Simoni et al., 2020). Changes in sediment and water supplies to the channel network caused by forest harvesting may alter the susceptibility of debris flows triggered by mass movement of channel deposits (May, 2002; Jakob et al., 2005). In the areas affected by wildfire, changes in the rainfall-runoff process, such as generation of overland flow due to decreased infiltration rates, also increase the occurrence of debris flows originating in channels (Staley et al., 2017; McGuire et al., 2018; Rengers et al., 2020). Consequently, forest harvesting may increase debris flow occurrence by affecting various hydrological and geomorphological processes.

The type and mode of the primary sediment transport processes in headwater channels are strongly affected by channel gradient. Bedload transport is the predominant transport mechanism in gentler channel reaches, while debris flows dominate in steep channels (e.g.,  $>15^\circ$ ) (VanDine, 1985; Iverson, 1997; Gomi et al., 2002; Tillery and Rengers, 2019). Thus, sediment supply from hillslopes into channel networks after the forest harvesting may not directly or immediately increase debris-flow risk in gentler channels. Both the contributing catchment area and the entry angle of landslides into the channel also affect initiation and mobility of debris flows (Benda and Cundy, 1990; Imaizumi and Sidle, 2007; Brayshaw and Hassan, 2009). Because a portion of the sediment displaced by landslides is deposited on hillslopes before reaching channels (Dymond et al., 1999, Imaizumi and Sidle, 2007), the connection of sediment transport processes between hillslopes and the channel network needs to be elucidated to ascertain the impact of forest harvesting on debris flow initiation.

The overall objective of this research is to reveal the combined effects of forest harvesting, subsequent forest regeneration, topography, and channel configuration on the occurrence of debris flows. We focus on debris flows that are directly or indirectly triggered by landslides, rather than debris flows that are only triggered by changes in rainfall-runoff processes in the basin. The history of debris flows was assessed using aerial photographs in the Sanko catchment, Japan, where forest management has been conducted for more than 100 years. The effects of terrain on temporal changes in susceptibility of debris flows after forest harvesting was also assessed by GIS terrain analyses. This approach allowed us to assess how forest management affected the timing and extent of debris flow occurrence.

## Study site

The Sanko catchment (area = 8.50 km<sup>2</sup>) is in the headwaters of the Kanno River, a tributary of the Kumano River, Japan (Fig. 1). Elevation within the study site ranges from 750 to 1372 m a.s.l. The geology of this area is dominated by a Cretaceous accretionary prism composed of sandstone and claystone called the Shimanto group. Bedrock in this group has been weakened due to fracturing and thrust formation. Sandstone is the dominant surface geology and is relatively homogeneous throughout the catchment. Channel gradients range from 1.5 to 5° in the main stem of the Kanno River, which flows from east to west through the middle of the catchment; tributaries have gradients of 5 to 35°. Hillslopes are steep throughout the catchment with a mean gradient of 34° (Fig. 1d). The east end of the catchment is relatively steeper than other areas. Valleys in the study site are V-shaped with narrow riparian areas (ranging from 5 to 10 m wide, except the main stem). Slope gradient in the lower portion of most hillslopes proximate to channels is approximately 40° or steeper. Soil depth typically ranges from 0.5 to 1.0 m.

Annual precipitation observed at Wakayama Forest Research Station located about 3 km west of the study site, is 2500 mm (Imaizumi, 2008). Heavy rainfall (i.e., total rainfall depth > 100 mm) occurs during the Baiu front from middle of June to late July and in the typhoon season from late August to October. Snowfall occurs at higher elevations within the study site, but precipitation from December to February is only about 10% of annual precipitation. Snow generally melts within one week and a seasonal snowpack does not persist.

A large extent of the Sanko catchment (about 95%) is covered with artificial (planted) conifer forest (Japanese cedar with minor amounts of Japanese cypress) under industrial management. The remainder is secondary deciduous broadleaf forests, log landings, and forest roads. Clearcutting is the only harvesting method employed in the

study site and replanting of nursery trees usually occurs one or two years after harvesting. Trees were cut with chainsaws throughout the period of landslide and debris flow assessments. Skyline logging, which transports logs by suspending them above ground using cables, has been main yarding method since the 1960's, while "chute yarding", which transports logs by sliding them on chutes made of logs, was conducted before that time. Since the timber harvest is typically conducted uniformly throughout each sub-catchment, both the harvesting and replanting periods are almost constant in each sub-catchment (Imaizumi et al., 2008). Thus, changes in debris flow frequency with increasing forest age (elapsed time after harvesting and replanting) can be analyzed in the Sanko catchment.

## **Methodology**

Location of debris flows and landslides in the study site were interpreted using aerial photographs for nine years (1964, 1967, 1971, 1976, 1984, 1989, 1994, 1998, and 2003). Scale of photographs, which are monochrome except those for 1976 (color photographs), ranged from 1:15,000 to 1:20,000. Most of the aerial photographs were taken in March prior to the rainy season. Therefore, almost all mass movements identified in aerial photographs likely occurred before autumn of the previous year – typically in the Baiu and typhoon seasons. Debris flows and landslides were visually identified in printed stereo photograph pairs using a stereoscope. Identified debris flows and landslides were mapped on 1:5000 forest management maps then analyzed using GIS. New mass movements were identified by comparing successive aerial photographs. Since it was difficult to classify the types of all mass movements (i.e., landslides and debris flows) based on field surveys due to the large number of events and the loss of evidence following sediment transport episodes, we classified the type of mass movements based on their location on aerial photographs. All mass movements on

hillslopes, mainly characterized as shallow translational landslides, were designated as landslides and all in-channel mass movements were designated as debris flows. Because our classification is not based on sediment transport mechanisms, some movements of landslide sediment in steep channels classified as debris flows may have occurred without being fluidized. Landslides were identified by the appearance of new bare areas on hillslopes or by the disruption of the regular pattern of trees, which were evenly replanted in the study site. Channel reaches affected by debris flows were interpreted based on accumulations of displaced planted trees along channels (Fig. 1c) because trees are not planted in the riparian areas and are not damaged by storm runoff in the absence of debris flows. One limitation of aerial photograph investigations is that they cannot be used to identify smaller landslides and debris flows because of the forest canopy; the threshold scale of non-visible mass movements depends on forest cover conditions (Brardinoni and Church, 2003; Brardinoni et al., 2003). Although smaller landslides may easily be obscured by mature forest canopies, the relationship between forest age and minimum size of landslides identified on aerial photographs (ranging appropriately 20–45 m<sup>2</sup>) was not clear in the Sanko catchment. Field surveys conducted in the study site revealed that landslides larger than 50 m<sup>2</sup> were likely to be detected on aerial photographs. High tree density ( $\geq 0.3$  trees per m<sup>2</sup>) and the regular pattern of the replanting in the Sanko catchment may have resulted in the small size of the detectable landslides on aerial photographs. Thus, we set a minimum size of landslides for analysis as 50 m<sup>2</sup> to prevent error caused by differential recognition of smaller landslides amongst photograph periods. Forest management records since 1913 were used to assess duration between forest harvesting and occurrence of landslides and debris flows. Landslides in the Sanko catchment typically occur at the bedrock surface or shallower depths, with an average depth of 0.6 m (Fig. 1b, Imaizumi et al., 2008). Debris flows

that did not displace trees cannot be identified in our interpretation of aerial photographs. Debris flows initiating from forest roads were excluded from the GIS analyses to focus specifically on the effects of clearcutting and subsequent replanting on debris flow occurrence. Given that forest roads in the catchment were largely located along ridgelines and valley bottoms, few debris flows initiated along these corridors.

Landslides were classified into three groups based on the progression of landslide sediment (Fig. 2): (1) landslides terminating on hillslopes; (2) landslide sediment that immediately stops at a channel junction; and (3) landslides directly evolving into debris flows. The lower elevation limits for the areas disturbed by landslide/debris flow sediment are the hillslope, hillslope-channel junctions, and channels, respectively. Some landslides may be misclassified when the lower portion of landslide sediment did not remove trees. Debris flows triggered by erosion of previously deposited landslide sediment are also classified as landslides directly evolving into debris flows (Fig. 2c) if the landslide and debris flow occurred in the same photograph period because of the difficulty in segregating them based on aerial photographs. Channel gradient at the landslide-channel junction for landslides reaching channels (Figs. 2b, 2c) was obtained from airborne LiDAR DEM (5 m resolution) provided by Geospatial Information Authority, Japan. To reduce errors in calculation of channel gradient derived from local roughness (e.g., large boulders and small-scale step topography of channel sections with exposed bedrock) and gaps in the LiDAR point cloud, channel gradient was calculated as the arctangent of elevation change within 20 m downstream of the channel junction divided by the section length (= 20 m). The junction angle between incoming landslides and the channel was interpreted using GIS ( $\theta$  in Fig 2).

Strahler stream order was also interpreted in GIS. Location of channel heads were mapped based on shape of contour lines on 1:5000 forest management maps. Before mapping, field surveys were conducted in sub-basins to check the shape of contour lines along the channel where fluvial transport dominates over diffusive transport. The channels with intermittent overland flow, consisting partly of zero order basins (Tsukamoto, 1963; Sidle et al., 2018), are also considered first-order basins in this study because of difficulty interpreting the existence of overland flow in all channels via field surveys.

Rainfall data from 1975 (when Gomadan station was established by Japan Meteorological Agency) to 2009 was used to analyze rainfall patterns causing landslides and debris flows. Although there is a break in monitoring during winter (usually from November to March), continuous data during the period of heavy rainfall (June to October) are available for all years.

The volume–area relationship for landslides within the study site was obtained from our field measurements in 11 landslide scars, including their initiation and transport zones (Imaizumi et al., 2008). The volume of all landslides was estimated by applying this relationship to landslide areas measured by GIS. The volume of landslide sediment reaching channels was estimated from the total volume of landslides reaching channels (Figs. 2b, 2c) multiplied by the ratio of total landslide sediment that reached channels. The ratio of sediment reaching channels (0.95) assessed in the Miyagawa Dam catchment, Japan (Imaizumi and Sidle, 2007), which has similar climate, geological, and topographic conditions as the Sanko catchment, was used to estimate volume of sediment supply into channels. The ratio, obtained by field measurement of landslide scars and landslide deposits, is high in this geological unit because of steep topography in the lower portion of the hillslope (Fig. 1d).

## Results

### *Debris flows directly initiated from landslides*

A total of 146 debris flows originated in the period from 1964 to 2002, including 74 debris flows originating directly from landslides and 72 debris flows that were caused by mass movement of channel deposits (Fig. 1, Supplemental material figure).

Frequency of landslides was greatest 1-5 yr after clearcutting and decreased with increasing forest age (Fig. 3a). Frequency of landslides reaching channels (Figs. 2b, 2c) exhibited similar temporal patterns as for all landslides in the Sanko catchment. Number of debris flows originating directly from landslides was also greatest 1-5 yr after clearcutting, but then declined at a slower rate up through 20 yr after harvesting, after which only 10 debris flows occurred (Fig. 3b).

Many of the landslides evolved directly into debris flows in steep channel reaches with small hillslope-channel junction angles, while landslides terminated at the hillslope-channel junctions in gentle channel reaches with large hillslope channel junction angles (Fig. 4a). The ratio of landslides that evolved directly into debris flows, obtained by the number of landslides that directly evolve into debris flows (Fig. 2c) divided by the total number of landslides reaching channels, was highest in steepest ( $> 35^\circ$ ) channel reaches, where 86% of the landslides directly evolved into debris flows (Fig. 4a,b). In channel reaches  $< 20^\circ$ , only 25% of the landslides evolved into debris flows. The ratio of landslides that directly evolved into debris flows is also affected by the channel-junction angle of the incoming landslide. A higher ratio of landslides evolved into debris flows when channel-junction angles were small (Fig. 4c). No landslides evolved into debris flows when the channel-junction angle was  $> 75^\circ$ .

Rainfall patterns also affect the occurrence of debris flows, but the hydrometeorological conditions for debris flow initiation vary from area to area (e.g.,

Zimmermann, 1990). In our study site, maximum daily precipitation in each photo period did not show a clear relationship with the ratio of landslides reaching channels or the ratio of landslides evolving into debris flows (Fig. 5a, 5c). In contrast, maximum hourly precipitation was positively correlated with both ratios (Fig. 5b, 5d). Although these relationships are not statistically strong because of the sparse data (p-value > 0.1 for both), they imply that short-term rainfall patterns affect the occurrence of debris flows.

### ***Debris flows caused by mass movement of channel deposits***

Landslides on hillslopes do not only directly evolve into debris flows, but also supply a large volume of sediment into channel networks. This deposited landslide material accumulates in the channel and can later be mobilized as a debris flow. Such debris flows caused by the mass movement of accumulated deposits within the channel was largest in the 10 yr period after harvesting; progressively less landslide sediment volume reached channels from 10 to 25 yr after harvesting (Fig. 6). Debris flow frequency originating in channels shows a similar time variation as the volume of landslide sediment reaching channels, except that debris flows declined substantially in the period from 5-10 yr after clearcutting, possibly due to lagged effects on debris flow initiation (Fig. 6). Debris flows originating in channels lasted for 25 yr after forest harvesting; no debris flow occurred after that. An important topographic factor affecting the initiation point of debris flows caused by mass movement of channel deposits is channel gradient (Fig. 7). Initiation points of 63 debris flows (88% of the total number of debris flows initiating directly within channels) were in channel reaches > 20°, while only nine debris flows initiated in channel reaches < 20°.

### ***Catchment topography and occurrence of debris flows***

Many debris flows in Sanko catchment initiated in first-order streams (Fig. 8, 9a). Of all debris flows, 92% of those that directly initiated from landslides and 86% of those originating in channels occurred in first-order streams. One of the important characteristics of first-order streams in this study area is the steep channel gradient; generally  $> 20^\circ$  (Fig. 9b, c). Channel junction angle differed from the upper to lower sections of a given channel (Fig. 9d). In first-order basins, the channel junction angle was generally smaller than in higher-order basins. Most of the debris flow initiation points that originated in channels larger than second-order received sediment supplied by landslides in their contributing areas, while many debris flow initiation points that originated in first-order channels did not receive landslide sediment from within their contributing catchments (Table 1).

### **Discussion**

Previous experimental and field-based studies revealed that increases in landslide frequency after forest harvesting are highly affected by decreases in the root strength of harvested trees (Sidle, 1992; Imaizumi et al., 2008; Schwarz et al., 2016; Vergani et al., 2017). Increased landslide occurrence on hillslopes results in more landslides reaching channels (Figs. 3a, 3b). Once landslide sediments terminate and stabilize on hillslopes (Fig. 2A), debris flows will probably not evolve from landslide deposits because the amount of overland flow on forested hillslopes (maximum of several millimeters during an event) is likely not sufficient to mobilize these deposits. Therefore, landslides reaching channels are much more effective in mobilizing debris flows. The landslide frequency in regenerating forests older than 25 yr (Fig. 3a) was similar to the landslide frequency observed in the older forests that had not been harvested since 1916 ( $0.43 \text{ km}^{-2} \text{ yr}^{-1}$ ; Imaizumi et al, 2008). Hence, although all sub-catchments within the study

site have experienced forest harvesting in the 20<sup>th</sup> Century, the frequency of landslides that directly evolved into debris flows in forests older than 25 yr is likely similar to those in unharvested forests.

The ratio of landslides that evolve into debris flows is strongly affected by catchment topography. The higher ratio of landslides reaching steep channels that evolved into debris flows (Fig. 4b) corresponds to previous reports that many debris flow initiation zones are located in steep channel sections (e.g., VanDine, 1985; Cousot and Meunier, 1996; Chen and Yu, 2011; Tillery and Rengers, 2019). In contrast, the smaller ratio of landslides that evolved into debris flows where the hillslope-channel junction angle was large (Fig. 4c) is because sediment mobility decreases when the flow path direction changes (Benda and Cundy, 1990; Imaizumi et al., 2007; Brayshaw and Hassan, 2009). We found that steep gradients and small junction angles typically occur in first-order streams rather than higher order basins (Fig. 9). Thus, many debris flows that directly originate from landslides initiate in first-order streams (Fig. 8).

Short-term rainfall intensity is also a potential factor affecting the occurrence of debris flows (Staley et al., 2013; Peng et al., 2015; Staley et al., 2017; Ma et al., 2019). The ratio of landslides reaching channels was high in the period with high maximum hourly rainfall (Fig. 5b). A similar trend was also found in Miyagawa Dam catchment in Japan (Imaizumi and Sidle, 2007). Because landslide sediment with high water content are more mobile compared to dry landslide sediment (Legros, 2002, Zou et al., 2017; Crosta et al., 2018), landslides that occur during intense storms likely travel longer distances. The higher ratio of landslides that directly evolved into debris flows during intense rainfall events also implies high mobility of landslide sediment during intense rainfall (Fig. 5d). Short-term rainfall intensity was more important than long-term rainfall (i.e., daily rainfall), likely because shallow landslides, which can be triggered by

rainfall in a short time period (Sidle and Swanston, 1982; Dai and Lee, 2001; Hattanji, 2003; Zêzere et al., 2015), dominate in the Sanko catchment (average landslide depth = 0.6 m; Imaizumi et al., 2008).

Some similarities in debris flow behaviour can be ascertained between the findings in our study and results from areas affected by wildfire, where changes in rainfall-runoff process in the catchment also affect the occurrence of debris flows (Cannon et al., 2001; Kean et al., 2011; Staley et al., 2017). Wildfires decrease the infiltration capacity of soils facilitating overland flow, which mobilize newly eroded and stored sediment in channels as debris flows (McGuire et al., 2018; Rengers et al., 2020). Hence, short-term rainfall intensity, which generates overland flow, is an effective rainfall threshold that controls post-wildfire debris flows originating in channels (Staley et al., 2017; McGuire et al., 2018; Rengers et al., 2020). Although differences in the rainfall-runoff characteristics were not clear among basins with different forest ages in Sanko catchment (Imaizumi et al., 2012), changes in stream discharge can affect the occurrence of debris flows in harvested areas.

Most debris flows originating in higher order streams (>2nd order), which have larger contributing areas than first-order streams, were influenced by sediment supplied by landslides in their contributing area (Table 1). Many mountainous basins are characterized as supply-limited (weathering limited) basins, in which the occurrence of debris flows is controlled by the volume of sediment in the channel supplied by landslides or other geomorphic processes in the system (Bovis and Jakob, 1999; Jakob et al., 2005; Theule et al., 2015). Therefore, increases in the volume of sediment supplied to channel networks after forest harvesting, also reported in earlier studies (May, 2002; Jakob et al., 2005; Hatten et al., 2018; Rachels et al., 2020), likely facilitated the occurrence of debris flows in higher-order basins of Sanko catchment. In

contrast, sediment supplied into the channel network by landslides is not as important in first-order streams because many debris flows occurred directly by landslides that mobilized from hollows, not from additional sediment transported from within the contributing area (Table 1).

Erosion rate by landslides, calculated from the volume of landslide sediment reaching channels in the period from 5-10 yr after clearcutting for the entire catchment ( $260 \text{ m}^3 \text{ km}^2 \text{ yr}^{-1}$ , Fig. 6), is  $0.26 \text{ mm yr}^{-1}$ . Annual bedload and suspended sediment yields measured in a sub-basin without recent landslides were  $0.09$  and  $0.12 \text{ kg m}^{-2} \text{ yr}^{-1}$ , respectively (Imaziumi et al., 2012). The estimated sediment yield from this sub-basin that was not recently managed is  $0.10 \text{ mm yr}^{-1}$ , assuming the volumetric weight of sediment =  $2000 \text{ kg m}^{-3}$ . Consequently, the increase in landslide frequency due to forest harvesting appear to increase the sediment supply rate into channel network by 2.6-fold, likely affecting debris flow frequency in channels (Fig. 6). Steepness of first-order valley bottoms often exceeds  $30^\circ$  (Fig. 9). Therefore, instability of channel banks and hollows, which are affected by decreased reinforcement of tree root networks after harvesting, likely triggered debris flows in first-order basins. Such directly connected landslides (in hollows) and debris flows (in first-order channels) are difficult to separate on aerial photographs.

The method of timber yarding (the transport of cut logs to the landing) can also affect sediment transport in mountain areas depending on the level of ground disturbance (e.g., Sidle, 1980; Roberts et al., 2004). In the Sanko catchment, the yarding method was changed from “chute yarding” to skyline yarding near the beginning of the period when landslide and debris flow occurrence was accessed (1960’s). Because damage to the forest floor by skyline logging is less than for chute yarding, this change

in the yarding method may have imposed a minor effect on the occurrence of debris flows.

### **Summary and Conclusion**

To clarify the impact of forest harvesting on the occurrence of debris flows, aerial photograph interpretations and GIS analysis were conducted in the Sanko catchment, central Japan, where forest management records are available from 1912. Our study showed that temporal changes in debris flow frequency after forest harvesting closely relates to the occurrence of landslides. Frequency of debris flows originating directly from landslides increases shortly after forest harvesting, especially in channels with steep gradients and small hillslope-channel junction angles. Ratios of landslides evolving into debris flows in first-order basins are higher than those in lower channel reaches, because many first-order channels have such geomorphic characteristics. Short-term rainfall intensity (1-h intensity) also affected the number of landslides that directly evolved into debris flows. Frequency of debris flows caused by mass movement of channel deposits increased after forest harvesting in steep channel sections. Sediment supply into channel networks by landslides is likely important in lower channel reaches, while instability of riparian areas (bank failures) and hollows may accelerate the occurrence of landslides and debris flows in upper channel reaches. Differences in debris flow activity after forest harvesting that manifest in different terrain indicate that harvesting areas should be carefully selected within managed forests based on topography to prevent sediment disasters following harvesting. Topography also needs to be considered when sediment disaster mitigation is implemented in harvested areas. Although this study mainly focused on the occurrence of debris flows associated with landslides, there are other factors affecting frequency of debris flows (e.g., active rill

and gully erosion, bank erosion, changes in hydrological processes). These factors, together with landslides, should be considered in comprehensive assessments of the debris flow risk in harvested areas.

### **Acknowledgements**

This study was supported by JSPS Grant Numbers 18H02235, 18K18917, and 19K01156. Professors Naoko Tokuchi, Nobuto Ohte, and Keitaro Fukushima kindly provided us with data on forest harvesting in the Sanko catchment. We appreciate Sanko Forestry, the owner of Sanko catchment, for allowing us access to the site and permission to conduct field surveys. Staff in Wakayama Forest Research Station kindly supported our study in the remote mountain area. Gratitude is also expressed to previous members of the Slope Conservation Section at the Disaster Prevention Research Institute, Kyoto University (Toshitaka Kamai, Takashi Gomi, Sohei Kobayashi, Rieko Kamei, and the other colleagues and students) for helping with this study. Professors Dieter Rickenmann and Masaharu Fujita kindly provided us with beneficial comments.

### **Declaration of Interest**

The authors declare that they have no known competing financial interests or personal relationships that could have appeared to influence the work reported in this paper.

### **References**

- Benda, LE, Cundy TW. 1990. Predicting deposition of debris flows in mountain channels. *Can Geotech J.* 27: 409–417.
- Bovis, M. J., Jakob, M., 1999. The roll of debris supply conditions in predicting debris flow activity. *Earth Surf Proc Land.* 24: 1039–1054.

- Brardinoni F, Hassan MA, Slaymaker HO. 2002. Complex mass wasting response of drainage basins to forest management in coastal British Columbia. *Geomorphology*. 49: 109–124.
- Brayshaw D, Hassan MA. 2009. Debris flow initiation and sediment recharge in gullies. *Geomorphology*. 109: 122–131.
- Chen CY, Yu FC. 2011. Morphometric analysis of debris flows and their source areas using GIS. *Geomorphology*. 129: 387–397.
- Crosta GB, De Blasio FV, Frattini P. 2018. Global Scale Analysis of Martian Landslide Mobility and Paleoenvironmental Clues. *J Geophys Res. – Planets*. 123: 872–891.
- Cannon SH, Kirkham RM, Parise M. 2001. Wildfire-related debris-flow initiation processes, Storm King Mountain, Colorado. *Geomorphology*. 39: 171–188.
- Coussot P, Meunier M. 1996. Recognition, classification and mechanical description of debris flows. *Earth-Sci Rev*. 40: 209–227.
- Dai FC, Lee CF. 2001. Frequency–volume relation and prediction of rainfall-induced landslides. *Eng Geol*. 59: 253–266.
- Dymond JR, Jesen MR, Lovell LR. 1999. Computer simulation of shallow landsliding in New Zealand hill country. *Int J Appl Earth Obs*. 1: 122–131.
- Fan L, Lehmann P, McArdell B, Or D. 2017. Linking rainfall-induced landslides with debris flows runout patterns towards catchment scale hazard assessment. *Geomorphology*. 280: 1–15.
- Gomi T, Sidle RC, Richardson JS. 2002. Understanding processes and downstream linkages of headwater systems. *BioScience*. 52: 905–916.
- Guthrie RH. 2002. The effects of logging on frequency and distribution of landslides in three watersheds on Vancouver island, British Columbia. *Geomorphology*. 43: 273–292.

- Hattanji T. 2003. Lag time-volume relationship on deep-seated landslides induced by rainfall, *J. Japan Soc. Erosion Control Eng.* 55(6): 74–77. Japanese with English abstract.
- Hatten JA, Segura C, Bladon KD, Hale VC, Ice GG, Stednick JD. 2018. Effects of contemporary forest harvesting on suspended sediment in the Oregon Coast Range: Alsea Watershed Study Revisited. *Forest Ecol Manag.* 408: 238–248.
- Imaizumi F. 2019. Effects of terrain on temporal changes in susceptibility of debris flows and associated hydrogeomorphic processes after forest harvesting, In proceedings of 7th International Conference on Debris-Flow Hazards Mitigation.
- Imaizumi F, Sidle RC. 2007. Linkage of sediment supply and transport processes in Miyagawa Dam catchment, Japan. *J Geophys Res Earth Surf.* 112: F3.
- Imaizumi F, Sidle RC. 2012. Effect of forest harvesting on hydrogeomorphic processes in steep terrain of central Japan. *Geomorphology.* 169: 109–122.
- Imaizumi F, Sidle RC, Kamei R. 2008. Effects of forest harvesting on the occurrence of landslides and debris flows in steep terrain of central Japan. *Earth Surf Proc Land.* 33: 827–840.
- Imaizumi F, Masui T, Yokota Y, Tsunetaka H, Hayakawa YS, Hotta N. 2019. Initiation and runout characteristics of debris flow surges in Ohya landslide scar, Japan. *Geomorphology.* 339: 58–69.
- Iverson RM. 1997. The physics of debris flows. *Rev Geophys.* 35: 245–296.
- Jakob M. 2000. The impact of logging on landslide activity at Clayoquot Sound, British Columbia. *Catena* 38: 279–300.
- Jakob M, Bovis M, Oden M. 2005. The significance of channel recharge rates for estimating debris-flow magnitude and frequency. *Earth Surf. Proc. Land.* 30: 755–766.

- Jordan, P. 2006. The use of sediment budget concepts to assess the impact on watershed of forestry operations in the southern interior of British Columbia. *Geomorphology* 79: 27–44.
- Kean JW, Staley DM, Cannon SH. 2011. In situ measurements of post - fire debris flows in southern California: Comparisons of the timing and magnitude of 24 debris - flow events with rainfall and soil moisture conditions. *J. Geophys. Res. Earth Surf.* 116: F04019.
- Kean JW, McCoy SW, Tucker GE, Staley DM, Coe JA. 2013. Runoff - generated debris flows: Observations and modeling of surge initiation, magnitude, and frequency, *J. Geophys. Res. Earth Surf.* 118: 2190–2207.
- Legros F. 2002. The mobility of long-runout landslides. *Eng. Geol.* 63: 301–331.
- Ma C, Deng J, Wang R. 2018. Analysis of the triggering conditions and erosion of a runoff-triggered debris flow in Miyun County, Beijing, China. *Landslides* 15: 2475–2485.
- May CL. 2002. Debris flows throughout different forest age classes in the central Oregon coast range. *J. A. Water. Resour. As.* 38: 1097–1113.
- McGuire LA, Rengers FK, Kean JW, Staley DM, Mirus BB. 2018. Incorporating spatially heterogeneous infiltration capacity into hydrologic models with applications for simulating post-wildfire debris flow initiation. *Hydrol. Process.* 32: 1173–1187.
- Montgomery DR., Schmidt KM, Greenberg HM, Dietrich WE. 2000. Forest clearing and regional landsliding. *Geology* 28: 311–314.
- Peng JB, Fan ZJ, Wu D, Zhuang JQ, Dai FC, Chen WW, Zhao C. 2014. Heavy rainfall triggered loess–mudstone landslide and subsequent debris flow in Tianshui, China. *Eng. Geol.* 184: 79–90.

- Rachels, AA, Bladon KD, Bywater-Reyes S, Hatten JA. 2020. Quantifying effects of forest harvesting on sources of suspended sediment to an Oregon Coast Range headwater stream. *Forest Ecol. Manag.* 466: 118123.
- Rengers FK, McGuire LA, Oakley NS, Kean JW, Staley DM, Tang H. 2020. Landslides after wildfire: initiation, magnitude, and mobility. *Landslides.* 17: 2631–2641.
- Roberts B, Ward B, Rollerson T. 2004. A comparison of landslide rates following helicopter and conventional cable-based clearcutting operations in the Southwest Coast Mountains of British Columbia, *Geomorphology* 61: 337–346.
- Sakals ME., Sidle RC. 2004. A spatial and temporal model of root cohesion in forest soils, *Can. J. For. Res.* 34: 950–958.
- Saito H, Murakami W, Daimaru H, Oguchi T. 2017. Effect of forest clear-cutting on landslide occurrences: Analysis of rainfall thresholds at Mt. Ichifusa, Japan. *Geomorphology* 276: 1–7.
- Schmaltz EL, Steger S, Glade T. 2017. The influence of forest cover on landslide occurrence explored with spatio-temporal information. *Geomorphology.* 290: 250–264.
- Sidle RC. 1980. Slope stability on forest land, *Pac. NW Ext. Publ. PNW209*, 23 p., Oregon State Univ., Corvallis.
- Sidle RC. 1992. A theoretical model of the effects of timber harvesting on slope stability. *Water Resour. Res.* 28: 1897–1910.
- Sidle RC, Gomi T, Tsukamoto Y. 2018. Discovery of zero - order basins as an important link for progress in hydrogeomorphology. *Hydrol. Process.* 32: 3059–3065. <https://doi.org/10.1002/hyp.13246>.
- Sidle RC, Ochiai H. 2006. *Landslides: Processes, Prediction, and Land Use.* Water Resources Monograph 18, American Geophysical Union: Washington, DC.

- Sidle RC, Swanston DN. 1982. Analysis of a small debris slide in coastal Alaska. *Can. Geotech. J.* 19(2): 167–174.
- Sidle RC, Wu W. 1999. Simulating the effect of timber harvesting on temporal and spatial distribution of shallow landslides. *Z. für Geomorphologie* 43: 185–201.
- Sidle RC, Ziegler AD, Negishi JN, Abdul Rahim N, Siew R, Turkelboom F. 2006. Erosion processes in steep terrain – Truths, myths, and uncertainties related to forest management in Southeast Asia. *Forest Ecol. Manag.* 224: 199–225.
- Simoni A, Bernard M, Berti M, Boreggio M, Lanzoni S, Stancanelli LM, Gregoretti C. 2020. Runoff - generated debris flows: Observation of initiation conditions and erosion-deposition dynamics along the channel at Cancia (eastern Italian Alps). *Earth Surf. Process. Landforms* 45: 3556–3571.
- Staley DM, Kean, JW, Cannon SH, Schmidt KM, Laber JL. 2013. Objective definition of rainfall intensity–duration thresholds for the initiation of post-fire debris flows in southern California. *Landslides*: 10: 547–562.
- Staley DM, Jacquelyn AN, Kean JW, Laber JL, Tillery AC, Youberg AM. 2017. Prediction of spatially explicit rainfall intensity–duration thresholds for post-fire debris-flow generation in the western United States. *Geomorphology*. 278: 149–162.
- Theule JI, Liébault F, Laigle D, Loye A, Jaboyedoff M. 2015. Channel scour and fill by debris flows and bedload transport. *Geomorphology*. 243: 92–105.
- Tillery AC, Rengers FK. 2019. Controls on debris - flow initiation on burned and unburned hillslopes during an exceptional rainstorm in southern New Mexico, USA. *Earth Surf. Proc. Land*. 45: 1051-1066.
- Tsukamoto Y. 1963. Storm discharge from an experimental watershed. *J. Japan. For. Soc.* 45(6): 186–190.

- Ueno K, Kurobe K, Imaizumi F, Nishii R. 2015. Effects of deforestation and weather on diurnal frost heave processes on the steep mountain slopes in south central Japan. *Earth Surf. Proc. Land.* 40: 2013–2025.
- VanDine DF, 1985, Debris flows and debris torrents in the southern Canadian Cordillera. *Can. Geotech. J.* 22: 44–62.
- Vergani C, Giadrossich F, Buckley P, Conedera M, Pividori M, Salbitano F, Rauch HS, Lovreglio R, Schwarz M. 2017. Root reinforcement dynamics of European coppice woodlands and their effect on shallow landslides: a review. *Earth-Sci. Rev.* 167: 88–102.
- Zêzere L, Vaz T, Pereira S, Oliveira SC, Marques R, Garcia RAC. 2015. Rainfall thresholds for landslide activity in Portugal: a state of the art. *Environ. Earth. Sci.* 73: 2917–2936.
- Ziegler AD, Negishi JN, Sidle RC, Noguchi S, Abdul Rahim N. 2006. Impacts of logging disturbance on hillslope saturated hydraulic conductivity in a tropical forest in Peninsular Malaysia. *Catena.* 67: 89–104.
- Zimmermann M. 1990. Debris flows 1987 Switzzrland: geomorphological and meteorological aspects. In: *Hydrologu in Mountainous Regions. II – Artificial Reservoirs, Water and Slopes*, IAHS Publ. no. 194: 387–393.
- Zou Z, Xiong C, Tang H, Criss RE, Su A, Liu X. 2017. Prediction of landslide runout based on influencing factor analysis. *Environ. Earth Sci.* 76: 723.

**Table 1** Number of debris flows that have and do not have landslides reaching the channel network within their contributing areas. Occurrence of landslides was interpreted for 10 years prior to timing of debris flows.

Stream order	Number of debris flows with landslides	Number of debris flows without landslides
1 <sup>st</sup> order	10	43
> 2 <sup>nd</sup> order	7	1

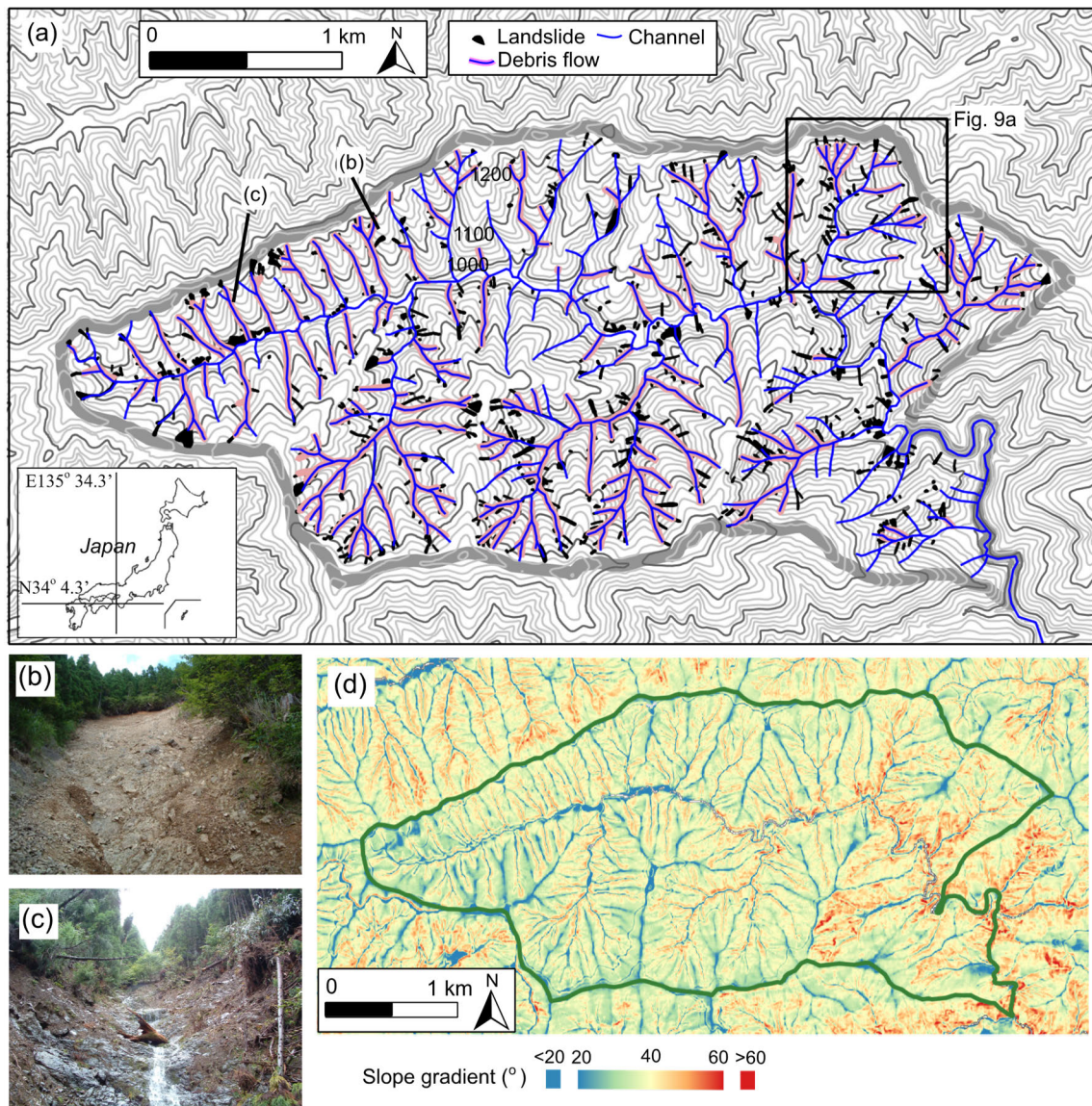


**Figure 1.** Topographic map and photographs of the Sanko catchment. (a) Topographic map and stream network for the 8.5 km<sup>2</sup> Sanko catchment, Japan. Landslides and debris flows identified in the aerial photographs from 1964 to 2003 are also shown in the figure. (b) Photograph of a landslide. Location of the photograph is shown in Fig. 1a. (c) Photograph of a channel scoured by a debris flow. (d) Spatial distribution of slope gradient.

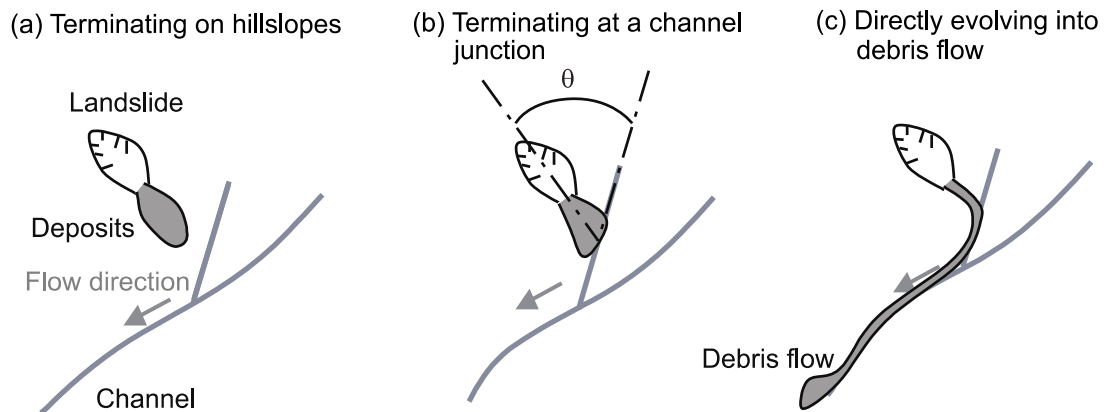


**Figure 2.** Classification of landslides based on the progression of landslide sediment: landslides terminating on hillslopes; landslides terminating at hillslope-channel junctions; and landslides that directly evolve into debris flows. The channel junction angle is illustrated as  $\theta$ .

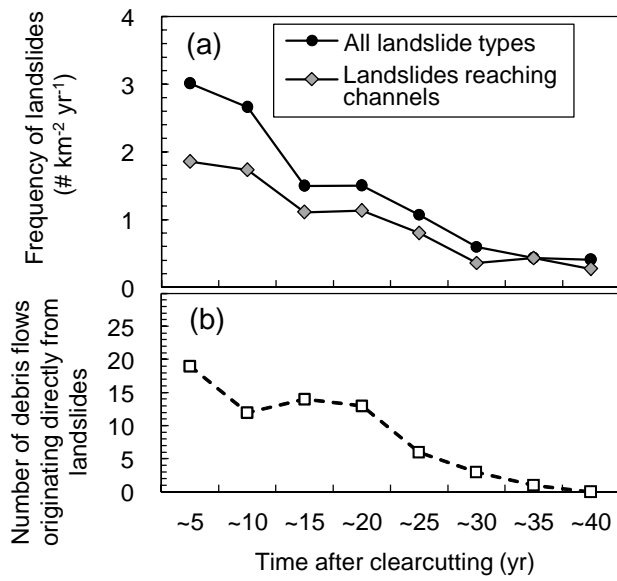


**Figure 3.** Temporal changes in frequencies of landslides and debris flows after clearcutting. (a) Frequency of all landslides and that of landslides reaching channels. (b) Number of debris flows originating directly from landslides (partly from Imaizumi et al., 2008).

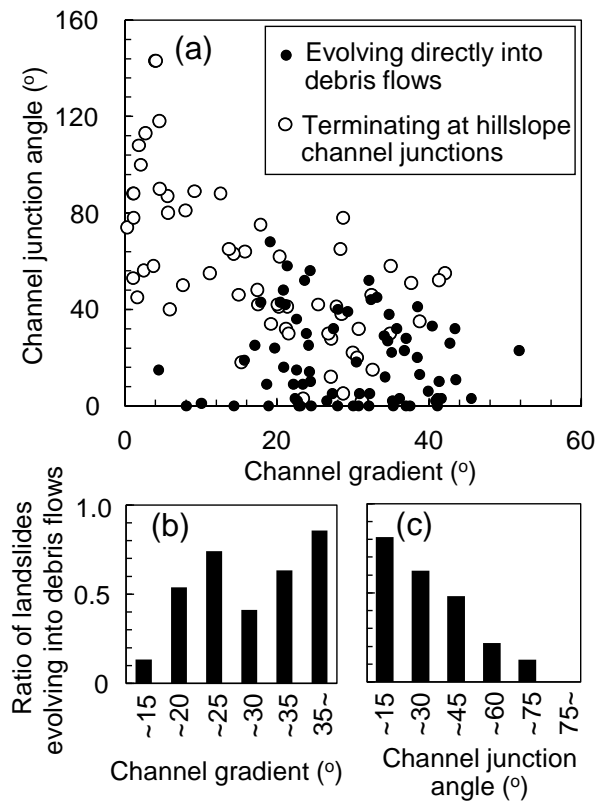


**Figure 4.** Topography at landslide-channel junctions. (a) Comparison between channel gradient and channel junction angle. (b) Ratio of landslides that evolve into debris flows in each channel gradient class. (c) Ratio of landslides that evolve into debris flows in each channel junction angle category.

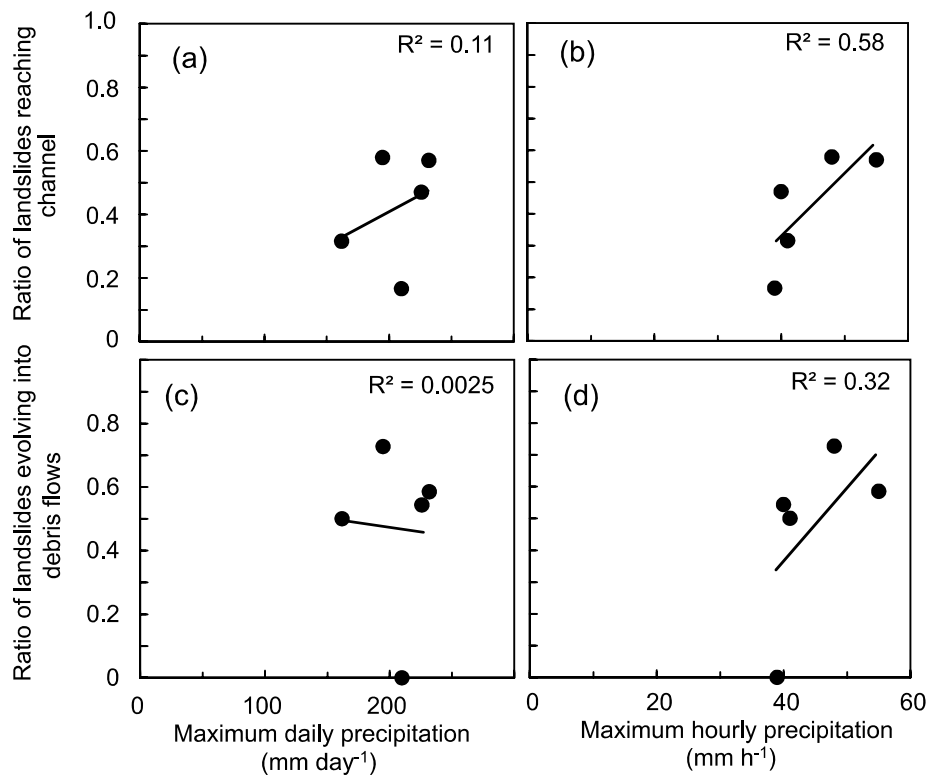


**Figure 5.** Relationships between rainfall intensities and mobility of landslide sediment.

(a) Comparison between maximum daily precipitation in each photo period and the ratio of landslides reaching channels. (b) Comparison between maximum hourly precipitation in each photo period and the ratio of landslides reaching channels. (c) Comparison between maximum daily precipitation and the ratio of landslides which entered streams that evolved into debris flows. (d) Comparison between maximum hourly precipitation and the ratio of landslides which entered streams that evolved into debris flows.

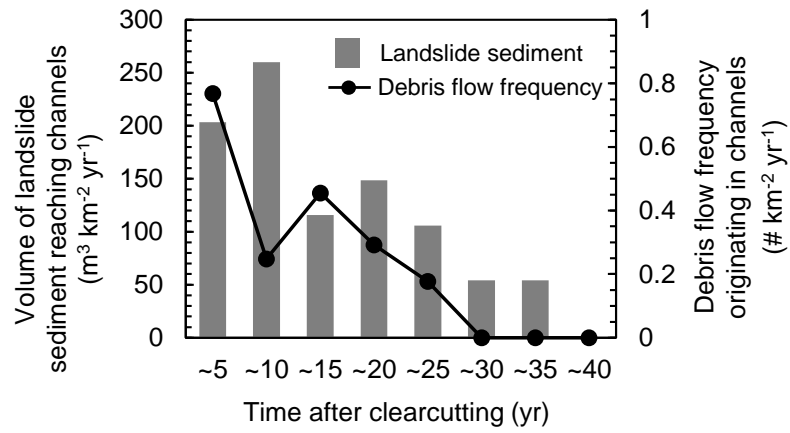


**Figure 6.** Temporal changes in the volume of landslide sediment reaching channels after forest harvesting (modified from Imaizumi et al., 2008 and Imaizumi, 2019).

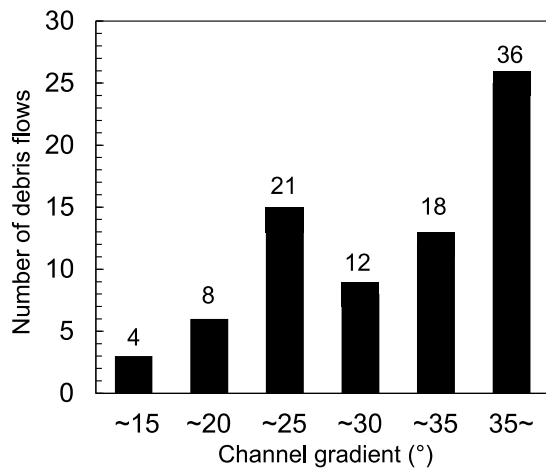


**Figure 7.** Number of debris flows originating in channels for each channel gradient class. Numbers above bars indicate the percentage of the total number of debris flows originating in channels.

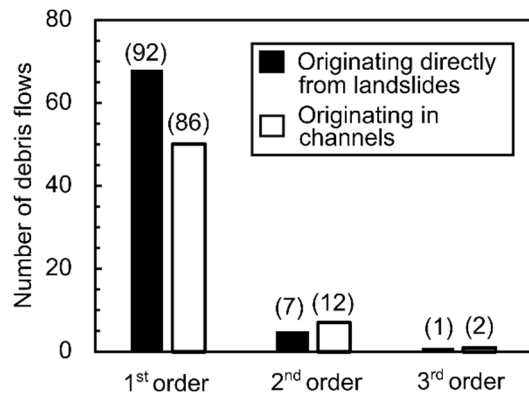


**Figure 8.** Number of debris flows initiating in various stream orders. Numbers above bars indicate the percentage of each initiation mechanism.

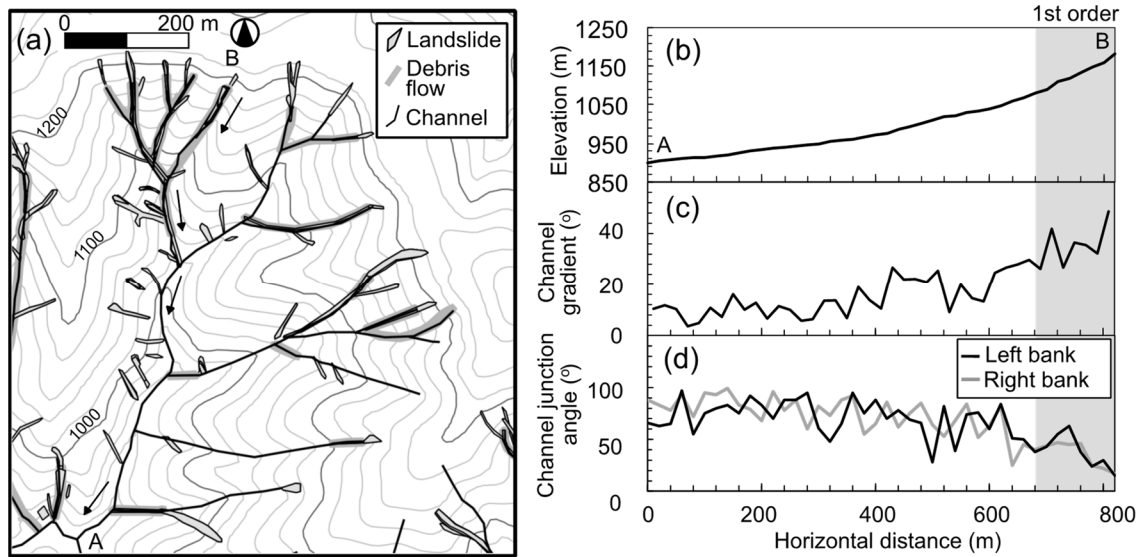


**Figure 9.** Spatial distribution of debris flows and longitudinal channel topography. (a) Spatial distribution of debris flows and landslides. Location of the map is shown in Fig. 1. (b) Longitudinal profile of channel topography in the section from A to B. (c) Longitudinal profile of channel gradient in the section from A to B. (d) Hillslope-channel junction angle in the section from A to B. The first order channel is shaded gray.

## Figure captions

**Figure 1.** Topographic map and photographs of the Sanko catchment. (a) Topographic map and stream network for the 8.5 km<sup>2</sup> Sanko catchment, Japan. Landslides and debris flows identified in the aerial photographs from 1964 to 2003 are also shown in the figure. (b) Photograph of a landslide. Location of the photograph is shown in Fig. 1a. (c) Photograph of a channel scoured by a debris flow. (d) Spatial distribution of slope gradient.

**Figure 2.** Classification of landslides based on the progression of landslide sediment: landslides terminating on hillslopes; landslides terminating at hillslope-channel junctions; and landslides that directly evolve into debris flows. The channel junction angle is illustrated as  $\theta$ .

**Figure 3.** Temporal changes in frequencies of landslides and debris flows after clearcutting. (a) Frequency of all landslides and that of landslides reaching channels. (b) Number of debris flows originating directly from landslides (partly from Imaizumi et al., 2008).

**Figure 4.** Topography at landslide-channel junctions. (a) Comparison between channel gradient and channel junction angle. (b) Ratio of landslides that evolve into debris flows in each channel gradient class. (c) Ratio of landslides that evolve into debris flows in each channel junction angle category.

**Figure 5.** Relationships between rainfall intensities and mobility of landslide sediment. (a) Comparison between maximum daily precipitation in each photo period and the ratio of landslides reaching channels. (b) Comparison between maximum hourly precipitation in each photo period and the ratio of landslides reaching channels. (c) Comparison between maximum daily precipitation and the ratio of landslides which entered streams that evolved into debris flows. (b) Comparison between maximum hourly precipitation and the ratio of landslides which entered streams that evolved into debris flows.

**Figure 6.** Temporal changes in the volume of landslide sediment reaching channels after forest harvesting (modified from Imaizumi et al., 2008 and Imaizumi, 2019).

**Figure 7.** Number of debris flows originating in channels for each channel gradient class. Numbers above bars indicate the percentage of the total number of debris flows originating in channels.

**Figure 8.** Number of debris flows initiating in various stream orders. Numbers above bars indicate the percentage of each initiation mechanism.

**Figure 9.** Spatial distribution of debris flows and longitudinal channel topography. (a) Spatial distribution of debris flows and landslides. Location of the map is shown in Fig. 1. (b) Longitudinal profile of channel topography in the section from A to B. (c) Longitudinal profile of channel gradient in the section from A to B. (d) Hillslope-channel junction angle in the section from A to B. The first order channel is shaded gray.